Absolute rate coefficients over extended temperature ranges and mechanisms of the CF($X^2\Pi$) reactions with F_2, Cl_2 and O_2

B. Vetters, B. Dils,† T. L. Nguyen, L. Vereecken,* S. A. Carl* and J. Peeters*

Received 11th November 2008, Accepted 20th February 2009
First published as an Advance Article on the web 23rd March 2009
DOI: 10.1039/b819984a

The absolute rate coefficients of the reactions of the carbyne-radical CF($X^2\Pi$, $\nu = 0$) with O_2, F_2 and Cl_2 have been measured over extended temperature ranges, using pulsed-laser photodissociation–laser-induced fluorescence (PLP–LIF) techniques. The CF($X^2\Pi$) radicals were generated by KrF excimer laser 2-photon photolysis of CF_2Br_2 at 248 nm and the real-time exponential decays of CF($X^2\Pi$, $\nu = 0$) at varying coreactant concentrations, in large excess, were monitored by LIF ($A^2\Sigma^+$, $\nu' = 1 \leftarrow X^2\Pi$, $\nu'' = 0$ transition). The experimental bimolecular rate coefficients of the CF($X^2\Pi$) reactions with F_2 and Cl_2 can be described by simple Arrhenius expressions: $k_{F2}(295–408\ K) = (1.5 \pm 0.2) \times 10^{-11} \exp[-(370 \pm 40)K/T]\ cm^3\ molecule^{-1}\ s^{-1}$; and $k_{Cl2}(295–392\ K) = (6.1 \pm 2.1) \times 10^{-12} \exp[+(280 \pm 120)K/T]$. The $k_{F2}(T)$ and $k_{Cl2}(T)$ results can be rationalized in terms of direct halogen-atom abstraction reactions in which the radical character of CF dominates; a quantum chemical CBS-Q//BHandHLYP/6-311G(d,p) study confirms that the ground state reactants CF($X^2\Pi$) + $F_2(X^1\Sigma)$ connect directly with the ground-state products $CF_2(X^1A_1)$ + $F(^2P)$ *via* a nearly barrierless F-atom abstraction route. The rate coefficient of CF($X^2\Pi$) + O_2 can be represented by a two-term Arrhenius expression: $k_{O2}(258–780\ K) = 1.1 \times 10^{-11} \exp(-850\ K/T) + 2.3 \times 10^{-13} \exp(500\ K/T)$, with a standard deviation of 5%. The first term dominates at higher temperatures T and the second at lower T where a negative temperature dependence is observed (<290 K). Quantum chemical computations at the CBS-QB3 and CCSD(T)/aug-cc-pVDZ levels of theory show that the $k_{O2}(T)$ behaviour is consistent with a change of the dominant rate-determining mechanism from a carbyne-type insertion into the O–O bond at high T to a radical–radical combination at low T.

Introduction

The small fluorocarbon radicals CF_x, x = 1–3, play a role in an array of chemical systems such as the atmosphere (CF_3 and its CF_3O product from the chlorofluorocarbon degradation in the stratosphere), high-temperature pyrolysis (halon fire suppressants)[1,2] and fluorocarbon etching plasmas in microelectronics technologies.[3–5] The diversity of reactive species and their interactions makes these systems extremely complex. For technological applications, the determination of the rate coefficients of the reactions involved is a key requirement in the elucidation of the complete reaction systems, which in turn leads to the possibility of system control based on insight.

Whereas more recent work in this laboratory on CF_x kinetics addressed reactions of electronically excited $CF_2(a^3B_1)$[6–9] and of ground-state CF_3,[10] the present research revisits the reactivity of the CF($X^2\Pi$) carbyne radical, in particular its reactions with F_2, Cl_2 and O_2. In earlier studies, in which we investigated the room-temperature reactions of CF($X^2\Pi$) with the above molecules and with several atomic and radical species,[11,12] as well as CF reactions with unsaturated hydrocarbons between 294 and 455 K,[13] we found indications that CF generally reacts more like a radical, showing only little of the carbyne reactivity typified by CH, except in the (slow) CF cycloaddition to unsaturated hydrocarbons. We ascribed the weakened carbyne character of CF to the partial filling of the "vacant" carbon orbital by fluorine 2p–π back-donation, which also rationalizes the significantly higher C–F bond strength of CF[14] than the average for CF_4—contrary to the CH and CH_4 case. Earlier, James *et al*. had already invoked halogen back-donation to explain the weaker carbyne character of CCl and CBr compared to CH.[15]

As an expansion of our previous rate-constant determinations at room temperature,[11] the present work aims to determine the reactivity of CF towards F_2, Cl_2 and O_2 over the more extended temperature ranges in which these reactions are of practical relevance, *i.e*. about 300 to 400 K for the CF + F_2/Cl_2 reactions in fluorocarbon-plasma etching processes, but extending to higher temperatures for the CF + O_2 reaction of interest to fluorocarbon pyrolysis/oxidation processes. While the first objective was obtaining the kinetic data as such for their practical value, another, fundamental, goal was to gain more insight into the molecular mechanisms of these reactions and into the electronic properties of CF that dominate its reactivity towards these

Department of Chemistry, University of Leuven, Celestijnenlaan 200F, B-3001, Leuven, Belgium. E-mail: Luc.Vereecken@chem.kuleuven.be, Shaun.Carl@chem.kuleuven.be, Jozef.Peeters@chem.kuleuven.be
† Present address: Belgian Institute for Space Aeronomy, Ringlaan 3, B-1180, Brussels, Belgium.

molecules. Whereas in this respect a moderate temperature range was sufficient for the CF reactions with F_2 and Cl_2, as both exhibit only slight and clear-cut temperature dependences, the CF + O_2 reaction required study over a wider temperature range as its kinetics proved to be more complex.

As far as the authors are aware, no other group has studied these reactions at elevated temperatures. Tsai and McFadden did examine the CF + O_2 reaction, but only at room temperature, reporting that "CF does not react with O_2"[16]—unambiguously contradicted by our previous results[11] as well as by the present.

As in our earlier studies on CF reaction kinetics, the rate coefficients were determined under pseudo-first-order conditions, using pulsed laser photolysis (PLP) coupled with time-resolved laser-induced fluorescence (LIF).

Experimental setup

The apparatus as well as the experimental procedures have been previously described and discussed in much detail,[11–13,17] thus only a brief summary is given here. Ground-state CF radicals were generated by 2-photon photodissociation of CF_2Br_2 at 248 nm, using a pulsed KrF excimer laser ($E_p \approx 200$ mJ per pulse, $\tau_p \approx 20$ ns). An extensive study covering all major aspects of this process was reported earlier.[17] In the present work, the beam section of the excimer laser was reduced to 8 mm × 2 mm by cylindrical optics before passing through the blackened stainless-steel LIF cell. Time-resolved probing of the CF($X^2\Pi$, $\nu'' = 0$) radicals was achieved by exciting the strong P_{11} band head of the $A^2\Sigma^+ \leftarrow X^2\Pi$ (1,0) transition using a pulsed dye laser tuned at 223.88 nm ($E_p \approx 1$–2 mJ per pulse, $\tau_p \approx 10$ ns, bandwidth ≈ 0.2 cm^{-1}), pumped by a Nd : YAG laser, and collecting the resulting A → X (1,6) band fluorescence at right angles with the probe laser and excimer laser beam axes, through a 0.22 m double-grating monochromator tuned to 268.4 ± 3.0 nm onto a photomultiplier tube (PMT). The delay t between the CF-generating photodissociation pulse and the CF-probe laser pulse, both with repetition frequencies of 10 Hz, was increased step-wise by a microprocessor-based digital delay generator (0.1 μs resolution). CF decays were usually monitored over a few ms, requiring some 2000 successive laser shots. The resulting CF signal decay as a function of time was recovered by an SRS boxcar integrator. Data acquisition and data reduction was achieved by PC. The total gas flow (~300 to 1500 cm^3 min^{-1} at total pressures from 2 to 10 Torr) was sufficient to refresh the mixture in the irradiated and observed volume (*ca.* 20 mm^2 × 10 mm) between successive laser shots, but slow enough to keep convective CF loss negligible compared to the reactive CF removal processes. The gases were fed to the reaction cell by calibrated mass-flow controllers. The concentrations of the various species were determined from their fractional flows and from the total pressure. A mixture of 43.4% CF_4 in ultra-high purity (UHP) He was used as the bath gas, while a mixture of 5% CF_2Br_2 in UHP He served as the CF precursor. CF_4 acts as an efficient quencher of vibrationally hot CF-radical photoproducts, with overall quenching constant k_q for $\nu'' \geq 1 \rightarrow \nu'' = 0$ relaxation estimated at $\approx 2 \times 10^{-13}$ molecule^{-1} cm^3 s^{-1}, based on our earlier room-temperature results.[11] Other gas mixtures used were 5% F_2 in He, 1.5% Cl_2 in Ar and 10% O_2 in He, all of high to ultra-high purity.

The reaction cell could be resistively heated up to a temperature of 900 K. However, in the presence of F_2 and Cl_2, temperature was kept below 450 K to minimize corrosion of reactor cell components. The temperature in the observed reaction volume was measured by a movable chromel–alumel thermocouple. Once a stable temperature was reached, the thermocouple was pulled back from the reaction volume.

Results

The CF LIF-signal decays were obtained under pseudo-first-order conditions at large excess of the molecular coreactant. The coreactant concentrations ranged between 10^{14} to 3 × 10^{16} molecule cm^{-3} and were varied over at least one order of magnitude, while the initial concentration of CF radicals was estimated to be $\sim 10^{10}$ molecule cm^{-3} from the observed signal magnitude and the known sensitivity of the detection equipment. The pseudo-first-order rate constants, k', were derived from the slopes of the plots of ln(signal-baseline) as a function of the delay time t between the excimer laser and probe laser pulses: $k' = -\mathrm{d}\ln[\mathrm{CF}(\nu'' = 0)]/\mathrm{d}t$. The CF($(\nu'' = 0)$ decays closely obey an exponential law, generally over three to four 1/e lifetimes. The signals at reaction times $t \rightarrow \infty$ correspond exactly to the baseline obtained by switching off the excimer laser or the PMT supply.[11–13] Examples of CF($\nu'' = 0$) decays by F_2, Cl_2 and O_2 have been shown earlier.[11] Initial portions of the ln[CF($\nu'' = 0$)] *versus* t plot that still show some curvature, because not all CF radicals are relaxed to the $\nu'' = 0$ ground state, are ignored in determining k'. As discussed earlier in detail,[11,13] CF_4 bath gas enhances CF($\nu'' \geq 1 \rightarrow \nu'' = 0$) vibration relaxation, compressing it, at partial pressure of *ca.* 4 Torr, into the first ≈50 μs, thus rendering the effects of vibrational relaxation on CF($\nu'' = 0$) decays negligible at longer t. The slope k' of the ln(signal-baseline) *vs.* t plots was derived by a least-squares fit routine with weights inversely proportional to the local signal noise.

The decay constants k' can be described by the sum:

$$k' = k[\text{coreactant}] + k_{\text{conv}} + k_{\text{diff}} + k_R[R]$$

in which k is the bimolecular rate constant of interest; k_{conv} the rate coefficient for convective removal; k_{diff} the rate constant for diffusion out of the probed volume; and k_R the bimolecular rate constant for the reaction of CF with species R other than the coreactant. The precursor concentration [CF_2Br_2] was typically about 3 × 10^{12} molecule cm^{-3} and was kept constant during a k determination, as were the laser-beam intensities, the total gas flow rate and the total pressure. Only the coreactant concentration was varied. Thus, plotting the obtained k' as a function of [coreactant] yields a straight line with slope equal to the bimolecular rate constant k and an intercept equal to $k_{\text{conv}} + k_{\text{diff}} + k_R[R]$. Again a weighted least-squares fitting procedure was used. An example of such a plot is shown in Fig. 1. The results for the rate coefficients k of the reactions of CF with F_2, Cl_2 and O_2 are listed in

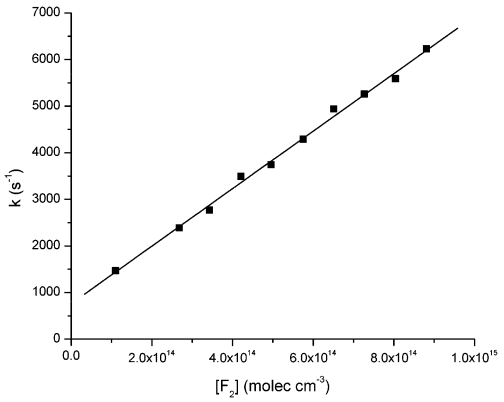

Fig. 1 Pseudo-first-order rate constant k' *versus* $[F_2]$ for the CF + F_2 reaction; T = 408 K; pressure = 10 Torr; He–CF_4 mixture bath gas. Statistical standard errors are of similar size as the symbols; absolute systematic error is estimated at 10%.

Table 1 CF + F_2 reaction; rate coefficient k as a function of temperature. The stated uncertainty is essentially the estimated 10% systematic error

T/K	$k/10^{-12}$ cm^3 s^{-1}
295	4.41 ± 0.45
295	4.32 ± 0.49
340	5.23 ± 0.54
371	5.48 ± 0.56
392	6.21 ± 0.64
408	6.08 ± 0.62

Table 2 CF + Cl_2 reaction; rate coefficient k in function of temperature. The stated uncertainty is essentially the estimated 10% systematic error

T/K	$k/10^{-11}$ cm^3 s^{-1}
295	1.59 ± 0.16
340	1.34 ± 0.14
372	1.42 ± 0.15
392	1.18 ± 0.13

Table 3 The CF + O_2 reaction; k as a function of temperature. The stated uncertainty is essentially the estimated 10% systematic error

T/K	$k/10^{-12}$ cm^3 s^{-1}
258	1.95 ± 0.20
294	1.69 ± 0.17
330	1.76 ± 0.18
378	2.04 ± 0.20
412	2.25 ± 0.23
455	2.43 ± 0.24
533	3.04 ± 0.30
563	2.72 ± 0.27
608	3.23 ± 0.32
695	3.55 ± 0.36
780	4.32 ± 0.43

Tables 1–3. While statistical standard deviations on the k values are mostly $\leq$ 3%, systematic errors, due mainly to inaccuracies in absolute coreactant concentrations and residual vibration relaxation effects, are estimated at about 10% and make up the bulk of the overall uncertainties listed.

Reaction with F_2

The reaction of CF with F_2 had already been determined in this laboratory at 294 K between 2 and 10 Torr. No pressure dependence could be observed, and a k_{F2} value of (3.9 ± 0.4) × 10^{-12} cm^3 molecule^{-1} s^{-1} was obtained.[11] Our present k_{F2}(295 K) of (4.41 ± 0.45) × 10^{-12} cm^3 molecule^{-1} s^{-1} is in agreement with this earlier result. To check whether the small fraction of F_2 molecules dissociated by the excimer laser pulse (estimated at 0.7% for a typical laser fluence of ≈10^{18} photons cm^{-2}) influence the obtained CF + F_2 rate coefficient value, experiments were run with the excimer laser fluence decreased by one order of magnitude. No appreciable difference in obtained rate coefficients was observed (k = (4.32 ± 0.49) × 10^{-12} cm^3 molecule^{-1} s^{-1}, see Table 1), clearly indicating that F atoms from F_2 dissociation have a negligible impact on the observed rate constant. The measured k_{F2} in the 295–408 K range are listed in Table 1. Fitting the data by a standard Arrhenius expression (see Fig. 2) yields:

$$k_{F2} = (1.5 \pm 0.2) \times 10^{-11} \times \exp(-(0.74 \pm 0.1)\ \text{kcal mol}^{-1}/RT)\ \text{cm}^3\ \text{s}^{-1} \quad (1)$$

Reaction with Cl_2

As with F_2, the reaction rate of CF with Cl_2 had already been determined in this laboratory at 296 K between 2 to 10 Torr. Also for this reaction, no pressure dependence was observed earlier and the reported[11] room-temperature rate constant k_{Cl2} = (1.7 ± 0.2) × 10^{-11} cm^3 molecule^{-1} s^{-1} is well reproduced by the present value of (1.59 ± 0.16) × 10^{-11} cm^3 molecule^{-1} s^{-1}. Note that the Cl_2 content of the commercial 1.5% Cl_2 in Ar mixture used in the present work was verified by passing a known flow through a KI solution over a known period of time, and titrating the I_2 formed with NaS_2O_3, so measuring a 1.55% Cl_2 content. The rate coefficients measured over the 295–392 K range, listed in Table 2, show a slight negative T-dependence. In our earlier 294 K study,[11] we found indications that interaction of Cl_2 with vibrationally excited CF($\nu'' \geq 1$) results more easily in CF($\nu'' \geq 1 \rightarrow \nu'' = 0$) relaxation than in chemical reaction.

An Arrhenius fit (see Fig. 2) yields:

$$k_{Cl2} = (6.1 \pm 2.1) \times 10^{-12} \times \exp((0.56 \pm 0.25)\ \text{kcal mol}^{-1}/RT)\ \text{cm}^3\ \text{s}^{-1} \quad (2)$$

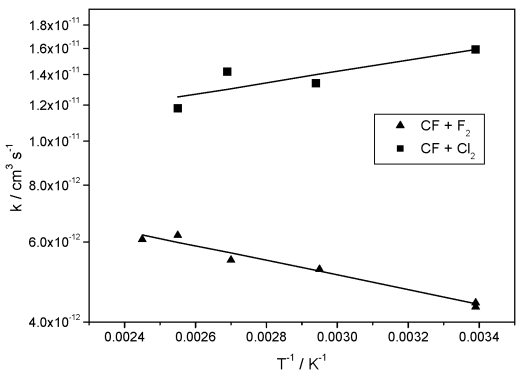

Fig. 2 Arrhenius plots of the rate coefficients k *versus* the inverse temperature T^{-1} for the reactions of CF + F_2 and CF + Cl_2.

Reaction with O_2

The CF + O_2 rate coefficient was determined over a wide temperature range, 258–780 K; the data are listed in Table 3. The room temperature value, $(1.69 \pm 0.17) \times 10^{-12}$ cm^3 molecule^{-1} s^{-1}, is again in good agreement with our previously determined $k = (1.6 \pm 0.2) \times 10^{-12}$ cm^3 molecule^{-1} s^{-1} in the 2–10 Torr pressure range, independent of pressure.[11] The $k_{O2}(T)$ data, depicted in the Arrhenius plot of Fig. 3, reveal a pronounced curvature, even exhibiting a change from a positive temperature dependence above 330 K to a negative one below 290 K. The data are well fitted by a sum of two independent Arrhenius expressions, as detailed in the Discussion section:

$$k_{O2} = 1.1 \times 10^{-11} \exp(-1.7 \text{ kcal mol}^{-1}/RT) + 2.3 \times 10^{-13} \exp(1.0 \text{ kcal mol}^{-1}/RT) \text{ cm}^3 \text{ s}^{-1} \quad (3)$$

It needs to be emphasized that our PLP–LIF results show unequivocally that CF exhibits a clear and precisely quantifiable reactivity towards O_2, thus unequivocally contradicting the earlier report by Tsai and McFadden[16] that "CF does not react with O_2". Moreover, our theoretical study (below) confirms a significant reactivity of CF toward O_2, requiring only slight activation.

Discussion

As stated above, one of the most interesting features of CF($X^2\Pi$) is that in principle it possesses carbyne properties: a vacant p-orbital combined with a lone pair, as well as radical properties. This means CF may undergo insertion and cycloaddition reactions typical for carbenes and carbynes such as $CH_2(a^1A_1)$ and CH($X^2\Pi$), but also abstraction or addition/recombination reactions typical for radicals. One of the prime reasons for undertaking this study over an extended temperature range was indeed to shed light on the mechanisms involved and to determine which of the two reaction types dominates.

CF + F_2

There are two *a priori* mechanisms by which this reaction might proceed. CF may insert into the F_2 σ-bond, forming vibrationally excited $CF_3^\dagger$ that promptly dissociates into ground state CF_2 + F:

$$CF(X^2\Pi) + F_2 \rightarrow CF_3^\dagger(X^2A_1) \rightarrow CF_2(X^1A_1) + F$$

Alternatively, CF could directly abstract an F atom from F_2 forming CF_2 and F:

$$CF(X^2\Pi) + F_2 \rightarrow CF_2(X^1A_1) + F$$

The carbyne-type insertion to form $CF_3^\dagger(X^2A_1)$ ($\Delta H_r(0\text{ K}) \approx -174$ kcal mol^{-1}) is more exothermal than direct F-abstraction ($\Delta H_r(0\text{ K}) \approx -86$ kcal mol^{-1}); however, insertion must proceed through a much tighter and therefore entropically and kinetically less favourable (variational) transition state. Moreover, carbyne insertion into a F–F bond should be strongly inhibited by the very low electron density of the F–F σ-bond induced by the high electronegativity of the F atoms (F_2 bond strength ≈38 kcal mol^{-1}, compared to ≈58 kcal mol^{-1} for Cl_2); this should hamper the initial electrophilic attack of a carbyne. Additionally, due to the partial occupation of the "vacant" carbon p-orbital through 2p–π back-donation from the fluorine atom,[11,12,15] CF($X^2\Pi$) is expected to show a much weaker *carbyne* reactivity than its unsubstituted CH($X^2\Pi$) counterpart. As shown in Table 4, the rate constant of CF + F_2 at 295 ± 5 K is found to be significantly higher than the k(CH + F_2) result of Nesbitt,[22] indicating that CF (and likely also CH) act as radicals in this reaction, with only a minor contribution of the carbyne-type channel. Comparison of our experimental rate constant of CF + F_2 at 295 ± 5 K [11] with those of typical radical + F_2 reactions (Table 4), clearly supports direct F-abstraction over carbyne-type insertion; according to the k(CH + F_2) value of Nesbitt[22] this applies also for CH + F_2.

A complementary quantum chemical study confirms that the CF($X^2\Pi$) + $F_2(X^1\Sigma)$ reaction proceeds *via* a direct F-abstraction mechanism in which CF behaves as a radical. An intrinsic reaction coordinate (IRC) analysis[18] at the CBS-Q[19]//BHandHLYP/6-311G(d,p)[20] level of theory (though adopting the more refined CBS-QB3 basis-set extrapolation scheme, affording an accuracy of a few kcal mol^{-1}—see ref. 21), shows that the ground-state reactants CF + F_2 connect directly to the ground-state products $CF_2(X^1A_1)$ + F(^{2}P) on a quasi-purely attractive potential-energy surface ("type-1" PES) without a marked energy barrier, as depicted in Fig. 4. On the other hand, all attempts to characterize a low-energy CF carbyne-type insertion into F_2 proved unsuccessful. When no geometry constraints are imposed, the pathways always revert to the direct F-abstraction route above, *i.e.* with the FC-carbon atom approaching F–F in a nearly collinear way. On the other hand, when *imposing* a C_s approach of FC perpendicular to the F–F bond so as to force an insertion, the CBS-Q//BHandHLYP/6-311G(d,p) PES (see Fig. 4) shows a high entrance barrier of at least 17 kcal mol^{-1}, before diving down to the −174 kcal mol^{-1} deep well of the $CF_3^\dagger(X^2A_1)$ intermediate that then fragments to $CF_2(X^1A_1)$ + F without an exit barrier. Thus, the theoretical results unequivocally show the direct FC–F–F abstraction route to be the dominant path.

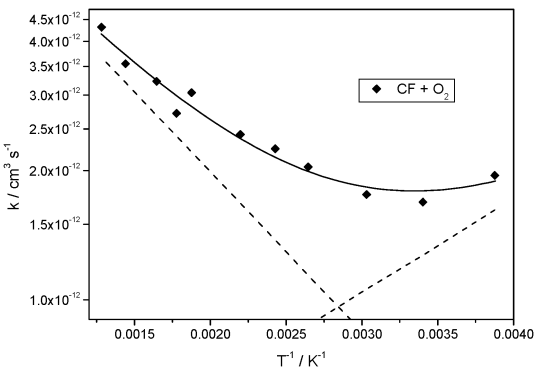

Fig. 3 Arrhenius plot of the bimolecular rate coefficient k of the reaction of CF with O_2 as a function of the inverse temperature T^{-1}. The solid curve (—) is a fit by a sum of two Arrhenius expressions (see text), the dashed lines (– – –) showing the two components.

Table 4 Rate coefficients at $T = 295 \pm 5$ K and Arrhenius parameters of CF reactions with F_2 and Cl_2 compared with literature values for the reactions of CH and of some typical radicals with F_2 and Cl_2

Reaction	$k_{295\pm5\ K}$/cm^3 s^{-1}	E_a/kcal mol^{-1}	$A_a/10^{-11}$ cm^3 s^{-1}	Ref.
CF + F_2	4.4×10^{-12}	0.7	1.5	This work
CH + F_2	1.9×10^{-12}	—	—	22
H + F_2	1.4×10^{-12}	2.1	5.0	23
CH_3 + F_2	1.0×10^{-12}	1.1	0.66	24
CF + Cl_2	1.6×10^{-11}	−0.6	0.61	This work
CH + Cl_2	1.5×10^{-10}	—	≈15	25
H + Cl_2	2.0×10^{-11}	0.8	8.0	26
CH_3 + Cl_2	2.0×10^{-12}	0.5	0.5	27
C_2H_5 + Cl_2	2.1×10^{-11}	−0.3	1.3	27

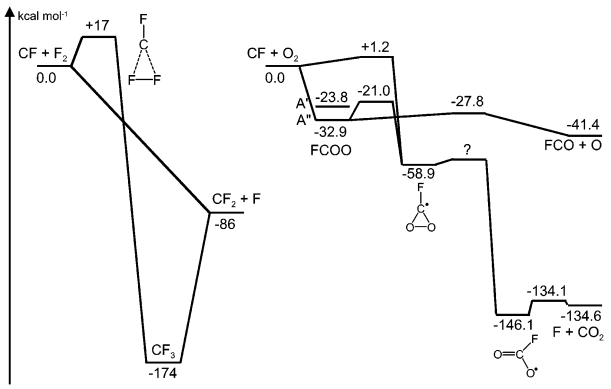

Fig. 4 ZPE-Corrected doublet potential-energy schemes for the reactions of CF + F_2 and of CF + O_2 (see text).

CF + Cl_2

Analogous with CF + F_2 the possible reaction pathways are:

$$CF + Cl_2 \rightarrow CFCl_2^{\dagger} \rightarrow CFCl + Cl$$

Here too, initial insertion, with $\Delta H_r(0\ K) \approx -84$ kcal mol^{-1}, would be far more exothermal than direct Cl-abstraction, $\Delta H_r(0\ K) \approx -24$ kcal mol^{-1}. Noteworthy is that, contrary to the reactions with F_2, the CH + Cl_2 reaction is one order of magnitude faster than its CF + Cl_2 counterpart (see Table 4), which is a strong indication of an insertion process in the CH + Cl_2 reaction. On the other hand, the rate of the slower CF + Cl_2 reaction compares strikingly well with those of typical radical + Cl_2 reactions.

Quantum chemical computations at reliable levels of theory for this system are very costly and outside of the scope of this work. However, the available experimental evidence (above) suggests that CF behaves as a radical in its reaction with Cl_2, as in that with F_2—which, moreover, shows a similar frequency factor A_a.

CF + O_2

The strong curvature of the Arrhenius plot, in particular for $T < 330$ K (see Fig. 3) is far too pronounced to be merely attributed to a temperature dependence of the pre-exponential factor. The most likely explanation for this unusual behaviour is a shift in the dominant reaction mechanism around 300 K. In contrast to the closed-shell F_2 and Cl_2 coreactants, $O_2(X^3\Sigma_g^-)$ is an open-shell biradical, allowing for a radical–radical combination reaction with the CF radical, which should be followed readily by expulsion of an O atom.

$$FC + O_2 \rightleftharpoons FCOO^{\dagger} \rightarrow FCO + O\ (\Delta H_r(0\ K) \sim -46\ \text{kcal mol}^{-1})$$

Radical recombination reactions in general are well known to be barrierless and to exhibit typically a negative temperature dependence due to an energy-dependent tightening of the transition state affecting the Arrhenius frequency factor. The negative temperature dependence observed in the $T < 300$ K range is indicative of such a barrierless reaction. At higher temperatures, $T > 330$ K, the temperature dependence of the rate constant becomes positive, indicative of a reaction with a small energy barrier. Given the carbyne character of CF, this reaction can be assumed to proceed *via* cycloaddition, followed by expulsion of the F atom:

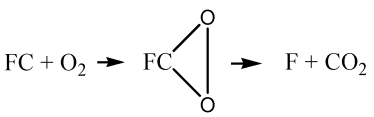

To further examine this atypical temperature dependence and characterize the distinct pathways, we performed exploratory quantum chemical calculations at the CBS-QB3 level of theory[21] on the [CFO_2] doublet potential energy surface; the resulting PES is shown in Fig. 4. The probable error of this level of theory is expected to be about ±2 kcal mol^{-1} for minima, but twice that for saddle-points. The FCOO chain-adduct formed in the radical–radical combination was found to have C_s symmetry with the radical electron located on the terminal oxygen. Two electronic structures were characterized: an A′ structure at −23.8 kcal mol^{-1} relative to the FC + O_2 reactants, and a more stable A″ structure at −32.9 kcal mol^{-1}. Upon scanning the end-to-end mutual approach of the CF + O_2 reactants, no evidence was found for an energy barrier between the reactants and the FCOO adduct; at large C–O separations >2 Å the calculations were perturbed by mixing with the quadruplet PES, obfuscating our efforts to characterize the entire kinetically relevant PES region. Starting from the most stable FCOO (A″) structure we located a dissociation transition state at −27.8 kcal mol^{-1} relative to the reactants, leading to the CFO + O products calculated at ≈−41.4 kcal mol^{-1} at this level of theory. We also located a cyclization transition state (−21.0 kcal mol^{-1}) for FCOO(A″) leading to a non-planar cyc-FCOO intermediate (C_s A′ symmetry, at −58.9 kcal mol^{-1}). Cyc-FCOO has the radical

electron located on the carbon in an sp^3 orbital, and has a fairly strained O–O bond with a length of 1.56 Å. Given that the cyclization TS is higher in energy and entropically much less favorable than the dissociation TS, it is expected that this latter channel is by far the dominant pathway for the FCOO chain-adducts.

However, the cyclic cyc-$FC(O_2)$ intermediate is also formed directly when the CF carbyne approaches the O_2 coreactant perpendicular to the O–O bond. CBS-QB3 predicts an energy barrier to cyclo-addition of $\approx$4.4 kcal mol^{-1} but fails to converge to a saddle-point transition-state structure. To improve our predictions on the cycloaddition transition state, we performed costly optimizations and frequency calculations at the CCSD(T)/aug-cc-pVDZ[28] level of theory, supplemented by CCSD(T)/cc-pVTZ single-point calculations, yielding a best estimate of +1.2 kcal mol^{-1} for the cycloaddition barrier. The resulting chemically activated cyc-$FC(O_2)$ is expected to promptly break its strained O–O bond, forming the planar FC(O)O (C_{2v} B_2 symmetry, −146.1 kcal mol^{-1}) stabilized by electron delocalization over the two oxygen atoms. FC(O)O in turn should easily expel the fluorine atom (TS at −134.1 kcal mol^{-1}) to form F + CO_2 (−134.6 kcal mol^{-1}). Finally, we also characterized the FOCO isomer (C_s A′ symmetry, −63.0 kcal mol^{-1}), but found no accessible pathways involving this intermediate.

The above results clearly support the proposed two-channel mechanism for the CF + O_2 reaction: a barrierless channel leading mainly to FCO + O prevailing at low temperatures, and a second channel with a barrier somewhat larger than 1 kcal mol^{-1} leading mostly to F + CO_2 becoming predominant at higher temperatures. The experimental data on the overall rate coefficient k_{tot} could indeed be fitted, with a standard deviation of only 5%, by a sum of the two Arrhenius expressions k_{cyc} and k_{rec} for each of these channels (see Fig. 3):

$$k_{O2} = k_{cyc} + k_{rec} = 1.1 \times 10^{-11} \exp(-1.7 \text{ kcal mol}^{-1}/RT) + 2.3 \times 10^{-13} \exp(1.0 \text{ kcal mol}^{-1}/RT) \text{ cm}^3 \text{ s}^{-1} \quad (4)$$

The Arrhenius parameters of the cycloaddition contribution, $A_a \pm \sigma_A = (1.1 \pm 0.3) \times 10^{-11}$ molecule^{-1} cm^3 s^{-1} and $E_a \pm \sigma_E = 1.7 \pm 0.7$ kcal mol^{-1} though showing a fairly large uncertainty due to statistical coupling with the two other fitting parameters, agree with our theoretical prediction of the barrier height for cycloaddition. The Arrhenius parameters for the radical–radical combination contribution have even larger errors as only a few data points are collected below the turnover point: $A = 2.3 \times 10^{-13}$ molecule^{-1} cm^3 s^{-1} with a statistical uncertainty of a factor 10, and $E_A = -1.0 \pm 1.2$ kcal mol^{-1}. A negative Arrhenius activation energy around −1 kcal mol^{-1} is typical for barrierless recombination reactions. The room-temperature rate coefficient of 1.7×10^{-12} molecule^{-1} cm^3 s^{-1} can be compared with that for O_2-addition reactions to delocalization-stabilized radicals such as allyl (6×10^{-13} molecule^{-1} cm^3 s^{-1})[29] and methyl-vinoxy (1.2×10^{-12} molecule^{-1} cm^3 s^{-1}).[30] The two-channel Arrhenius expression suggests the dominance of cycloaddition at temperatures >350 K, and primarily radical combination below that temperature.

Predicting the temperature- and pressure-dependent product distribution and rate coefficients *a priori* from the doublet [CFO_2] PES, *e.g.* using theories such as RRKM and Master Equation solvers, is outside the scope of this article. In particular, the proximity of the quadruplet PES and the existence of excited electronic states for some of the intermediates suggest the application of multi-reference quantum chemical methodologies to verify and refine the doublet potential energy surface for rigorous quantitative kinetic predictions. Moreover, the assumption of statistical distribution of the internal energy over all vibration modes, underlying the RRKM theory, is likely to break down for such small systems.

Conclusions

We have determined, for the first time, the absolute rate coefficients $k(T)$ of the reactions CF + F_2, CF + Cl_2, and CF + O_2 over extended temperature ranges. All these reactions are found to proceed at moderately high rates, showing only small T-dependences. The precise magnitudes of the rate coefficients and their T-dependences, compared with the corresponding data on analogous reactions of typical carbynes and radicals, strongly indicate that CF behaves in these reactions mainly as a radical, except in the reaction with O_2 at higher temperatures (>350 K), where cycloaddition becomes the dominant mechanism, as could be confirmed by complementary quantum chemical studies.

Acknowledgements

The authors are indebted to the FWO-Vlaanderen, the KULeuven Research Council (GOA program), and the Belgian Science Policy Office for continuing financial support. T.L. Nguyen thanks the KULeuven Research Council for a postdoctoral mandate. The assistance of Dr I. De Boelpaep is acknowledged for taking some of the decay measurements.

References

1 T. Noto, V. Babushok, A. Hamins and W. Tsang, *Combust. Flame*, 1998, **112**, 147.
2 B. A. Williams, D. M. L'Esperance and J. W. Fleming, *Combust. Flame*, 2000, **120**, 160.
3 M. J. Barela, H. M. Anderson and G. S. Oehrlein, *J. Vacuum Sci. Technol. A*, 2005, **23**, 408.
4 J. P. Booth, H. Abada, P. Chabert and D. B. Graves, *Plasma Sources Sci. Technol.*, 2005, **14**, 273.
5 D. Humbird and D. B. Graves, *J Appl. Phys.*, 2004, **96**, 2466.
6 B. Dils, S. A. Carl and J. Peeters, *Phys. Chem. Chem. Phys.*, 2003, **5**, 2376.
7 B. Dils, R. M. I. Elsamra, J. Peeters and S. A. Carl, *Phys. Chem. Chem. Phys.*, 2003, **5**, 5405.
8 B. Dils, R. M. Kulkarni, J. Peeters and S. A. Carl, *Phys. Chem. Chem. Phys.*, 2004, **6**, 2211.
9 T. L. Nguyen, S. A. Carl, M. T. Nguyen and J. Peeters, *J. Phys. Chem. A*, 2007, **111**, 6628.
10 B. Dils, J. Vertommen, S. A. Carl, L. Vereecken and J. Peeters, *Phys. Chem. Chem. Phys.*, 2005, **7**, 1187.
11 J. Peeters, J. Van Hoeymissen, S. Vanhaelemeersch and D. Vermeylen, *J. Phys. Chem.*, 1992, **96**, 1257.
12 J. Van Hoeymissen, I. De Boelpaep, W. Uten and J. Peeters, *J. Phys. Chem.*, 1994, **98**, 3725.

13 I. De Boelpaep, B. Vetters and J. Peeters, *J. Phys. Chem.*, 1997, **101**, 787.
14 A. P. Rendell, C. W. Bauschlicher and S. R. Langhoff, *Chem. Phys. Lett.*, 1989, **163**, 354.
15 F. C. James, H. K. J. Choi, B. Ruzsicska and O. P. Strausz, in *Frontiers of Free Radical Chemistry*, ed. W. A. Prior, Academic Press, NY, 1980, p. 139.
16 C. Tsai and D. L. McFadden, *J. Phys. Chem.*, 1989, **93**, 2471.
17 J. Van Hoeymissen, W. Uten and J. Peeters, *Chem. Phys. Lett.*, 1994, **226**, 159.
18 C. Gonzalez and H. B. Schlegel, *J. Chem. Phys.*, 1989, **90**, 2154.
19 J. W. Ochterski, G. A. Petersson and J. A. Montgomery, Jr, *J. Chem. Phys.*, 1996, **104**, 2598.
20 A. D. Becke, *Chem. Phys.*, 1993, **98**, 1372.
21 J. A. Montgomery, Jr, M. J. Frisch, J. W. Ochterski and G. A. Petersson, *J. Chem. Phys.*, 1999, **110**, 2822.
22 F. L. Nesbitt, PhD thesis, University of West Virginia, 1982.
23 V. V. Zelenov, A. S. Kukui, A. F. Dodonov, N. N. Aleinikov, S. A. Kashtanov and A. V. Turchin, *Khim. Fiz.*, 1991, **10**, 1121.
24 C. Seeger, G. Rotzoll, A. Lubbert and K. Schugerl, *Int. J. Chem. Kinet.*, 1981, **13**, 39.
25 S. M. Anderson, A. Freedman and C. E. Kolb, *J. Phys. Chem.*, 1987, **91**, 6272.
26 F. Berho, M.-T. Rayez and R. Lesclaux, *J. Phys. Chem. A*, 1999, **103**, 5501.
27 R. S. Timonen and D. Gutman, *J. Phys. Chem.*, 1986, **90**, 2987.
28 J. A. Pople, R. Krishnan, H. B. Schlegel and J. S. Binkley, *Int. J. Quant. Chem.*, 1978, **14**, 545.
29 M. E. Jenkin, T. P. Murrells, S. J. Shalliker and G. D. Hayman, *J. Chem. Soc., Faraday Trans.*, 1993, **89**, 433.
30 M. Hassouna, E. Delbos, P. Devolder, B. Viskolcz and C. Fittschen, *J. Phys. Chem. A*, 2006, **110**, 6667.